Plasmonic Properties and Photoinduced Reflectance of Topological Insulator

Zilong Wang[1,2], Jun Yin[1], Giorgio Adamo[2], Azat Sulaev[1], Lan Wang[1], Nikolay I. Zheludev[2,3] and Cesare Soci[1,2]

[1]*School of Physical & Mathematical Sciences, Nanyang Technological University, Singapore*
[2]*Centre for Disruptive Photonic Technologies, Nanyang Technological University, Singapore*
[3]*Optoelectronics Research Centre, University of Southampton, UK*
csoci@ntu.edu.sg

Abstract: We report on linear and nonlinear infrared and plasmonic properties of chalcogenide crystal of the Bi-Sb-Te-Se family that was recently identified as a prospective platform for switchable broadband plasmonic devices.

OCIS codes: (160.4670) Optical materials; (300.6340) Spectroscopy, infrared; (300.6380) Spectroscopy, modulation.

Topological insulator crystals are bulk insulators with robust conducting surface states protected by time-reversal symmetry, due to the strong spin-orbit coupling. Beyond their non-trivial electronic and lattice properties, which have been widely investigated for spintronic applications and quantum computation [1], topological insulators are also emerging optical materials for surface plasmonics [2]. Among the topological insulator single crystals, $Bi_{2-x}Sb_xTe_{3-y}Se_y$ (BSTS) shows superior properties of large bulk resistance and surface-dominated transport compared to more conventional bismuth binary compounds, such as Bi_2Se_3 and Bi_2Te_3 [3], as well as negative permittivity and low-loss plasmonic resonances in the visible and UV parts of the spectrum [2].

Here we present a study on the infrared spectroscopic characteristics of BSTS single crystals. The electronic bandgap energy and dielectric functions are obtained by first-principle density functional theory (DFT) and compared to the results of low-temperature linear and photoinduced transmittance and reflectance spectra under visible CW excitation.

$Bi_{1.5}Sb_{0.5}Te_{1.8}Se_{1.2}$ single crystals were synthesized by melting high-purity (99.9999%) Bi, Sb, Te and Se with molar ratio 1.5:0.5:1.8:1.2 at 950°C in an evacuated quartz tube. The temperature was then gradually decreased to room temperature over a span of three weeks. The BSTS crystal was then cleaved along the (100) family of planes to a thickness of ~0.5 mm [3].

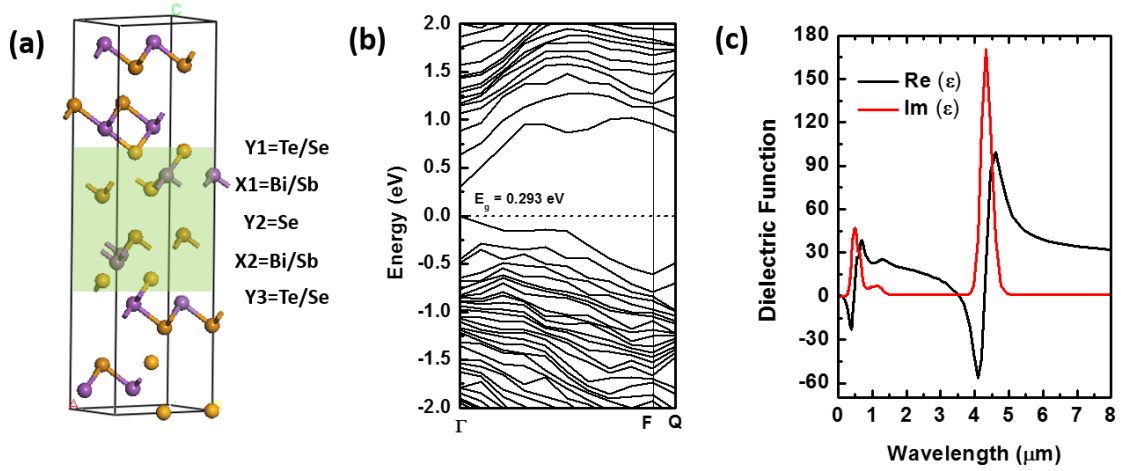

Fig. 1. Electronic and optical properties of $Bi_{1.5}Sb_{0.5}Te_{1.8}Se_{1.2}$ crystal obtained by DFT: (a) crystal structure of $Bi_{2-x}Sb_xTe_{3-y}Se_y$ ($y \geq 1$) compound; (b) electronic band structure and (c) real and imaginary parts of the dielectric function of super cell of $Bi_9Sb_3Te_{10}Se_8$ obtained by density function theory.

First-principle DFT calculations were carried out by generalized gradient approximation (GGA) with the Perdew-Burke-Ernzerhof (PBE) functional. Ultrasoft pseudopotentials were used to describe the electron-ion interactions of all elements. Integration over the Brillouin Zone was performed using a k-points grid of 4×4×4 during the super cell optimization and electronic properties calculations. The plane-wave basis set energy cutoff was

set to be 400 eV. The crystallographic structure of tetradymite chalcogenides $Bi_{2-x}Sb_xTe_{3-y}Se_y$ ($y \geq 1$) compound is shown in Fig 1 (a). The X_2Y_3 (X=Bi,Sb Y=Te,Se) cells have trigonal phase with R-3m symmetry. The model $Bi_9Sb_3Te_{10}Se_8$, which is close to the composition of $Bi_{1.5}Sb_{0.5}Te_{1.8}Se_{1.2}$, was arranged in the quintuple-like order along the c-axis. The resulting electronic band structure is shown in Fig. 1(b). The corresponding bandgap energy is found to be 0.293 eV, and decreases monotonically when increasing Bi and Te concentration. The dielectric function of BSTS was also calculated treating its imaginary part (ε_{Im}) as a response function within perturbation theory with adiabatic turning, where the dielectric tensor becomes the Drude-Lorentz one in the small adiabatic parameter. The real part (ε_{Re}) is derived from Kramers-Kronig transformation. The dielectric function shows two regions of anomalous dispersion in the UV-VIS and in the mid-IR, corresponding to the optical bandgap (Fig. 1(c)), suggesting that similar plasmonic effects as those recently observed in the UV-VIS region [2] may emerge in the mid-IR region as well.

Linear and photoinduced transmission and reflectance measurement were performed in a Fourier Transform Infra-Red (FTIR) spectrometer equipped with a liquid-nitrogen cooled cryostat (Fig.2). Both transmittance and reflectance show signatures of the optical bandgap around 0.3 eV, in agreement with the calculated value. Bandgap energy was determined by fitting the absorption coefficient with the formula $(\alpha h\nu)^2 \sim (h\nu - E_g)$ for direct interband transitions. The temperature dependence of the energy bandgap is found to follow the Varshni equation $E(\mathrm{T}) = E_0 - \alpha T^2/(T+\beta)$, with fitting parameters E_0 =0.316 eV, α =0.000245 eV/K, and β =58 eV. The corresponding optical bandgap at room temperature is ~0.256 eV, consistent with previously reported estimate [2].

Photoinduced reflectance ($\Delta R/R$) spectra were obtained by differential measurements with and without CW excitation at λ =532 nm. Besides the strong differential signal at the band edge region, reflectance modulation both above (enhancement) and below (reduction) the bangap energy are demonstrated throughout the near to mid-infrared region. This may be employed for broadband optical switching in reconfigurable plasmonic metamaterials.

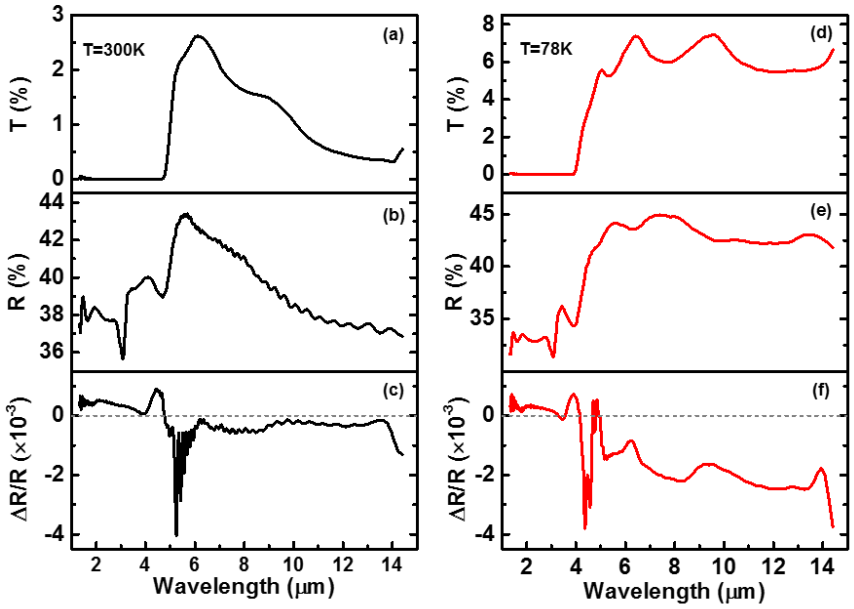

Fig. 2. Infrared transmittance (a,d), reflectance (b,e), and photoinduced reflectance (c,f) spectra of $Bi_{1.5}Sb_{0.5}Te_{1.8}Se_{1.2}$ measured at room temperature (left panels) and 78K (right panels).

In conclusion, we determined optical properties of topological insulator $Bi_{1.5}Sb_{0.5}Te_{1.8}Se_{1.2}$ single crystal by a combination of first-principle calculations and infrared spectroscopy. We provide temperature and stoichiometry dependence of the energy bandgap and demonstrate broadband photoinduced modulation across the near to mid-IR.

[1] J. E. Moore, The birth of topological insulators, Nature **464**, 194-198 (2010).
[2] J. K. S. J. Y. Ou, G. Adamo, A. Sulaev, L. Wang, and N. I. Zheludev, Ultraviolet and visible range plasmonics of a topological insulator, arXiv.org **1401.1415** (2014).
[3] B. Xia, P. Ren, A. Sulaev, P. Liu, S.-Q. Shen, and L. Wang, Indications of surface-dominated transport in single crystalline nanoflake devices of topological insulator, Physical Review B **87**, 085442 (2013).